

## Article

# The Use of Lightweight Penetrometer PANDA for the Compaction Control of Classified Sand Tailings Dams

Gabriel Villavicencio <sup>1,\*</sup>, Claude Bacconnet <sup>2,†</sup>, Pamela Valenzuela <sup>1</sup>, Juan Palma <sup>1</sup>, Alex Carpanetti <sup>3</sup>, Gonzalo Suazo <sup>4</sup>, Matías Silva <sup>5</sup> and José García <sup>1</sup>

<sup>1</sup> Grupo de Geotecnia, Escuela de Ingeniería de Construcción y Transporte, Pontificia Universidad Católica de Valparaíso, Avenida Brasil 2147, Valparaíso 2362804, Chile

<sup>2</sup> Institut Pascal, Université Clermont-Auvergne, BP 10448, F-63000 Clermont-Ferrand, France, CNRS, UMR 6602, F-63171 Aubière, France

<sup>3</sup> Escuela de Ingeniería Química, Pontificia Universidad Católica de Valparaíso, Avenida Brasil 2180, Valparaíso 2362804, Chile

<sup>4</sup> School of Civil Engineering, Universidad Técnica Federico Santa María, Avenida España 1680, Valparaíso 2390123, Chile

<sup>5</sup> Golder Associates, Las Condes, Magdalena 181, Santiago 7550055, Chile

\* Correspondence: gabriel.villavicencio@pucv.cl

† In memory of Claude Bacconnet.

**Abstract:** Sand tailings dams have historically been the most commonly used technology for tailings storage in Chile. Although engineering advances have resulted in the construction of approximately 250-m-high facilities, some operational challenges still remain, including compaction control. Control is currently performed at a few control points in a dam embankment, without considering a series of factors that affect its mechanical behavior (e.g., layer thickness and material variability). Within this context, geostatistics can be applied in combination with low-cost geotechnical tools as an alternative to improve compaction control in tailings storage facilities. In this study, an extensive field investigation was carried out. A total of 91 PANDA penetrometer tests were conducted to monitor the degree of compaction in an experimental classified sand tailings dam. The results were analyzed using stochastic interpolation for ordinary kriging and considering the spatial distribution of the cone resistance and the degree of compaction determined for the dam. The results showed that spatial variability was associated with the material variability of sand tailings and the compaction method used, and deviations from design requirements. The article shows the value of the use of geostatistics in decision-making in the case of classified sand tailings dams. This is mainly due to the fact that it allows optimization of the compaction process used in these tailings dams. Additionally, a useful database is generated to continue deepening studies of physical stability during the useful life of the tailings storage facilities.

**Keywords:** sand tailings dams; compaction control; variability; Lightweight Penetrometer PANDA



**Citation:** Villavicencio, G.; Bacconnet, C.; Valenzuela, P.; Palma, J.; Carpanetti, A.; Suazo, G.; Silva, M.; Garcia, J. The Use of Lightweight Penetrometer PANDA for the Compaction Control of Classified Sand Tailings Dams. *Minerals* **2022**, *12*, 1467. <https://doi.org/10.3390/min12111467>

Academic Editors: Masoud Zare-Naghadehi and Javad Sattarvand

Received: 13 October 2022

Accepted: 15 November 2022

Published: 20 November 2022

**Publisher's Note:** MDPI stays neutral with regard to jurisdictional claims in published maps and institutional affiliations.



**Copyright:** © 2022 by the authors. Licensee MDPI, Basel, Switzerland. This article is an open access article distributed under the terms and conditions of the Creative Commons Attribution (CC BY) license (<https://creativecommons.org/licenses/by/4.0/>).

## 1. Introduction

The Chilean Copper Commission (Comisión Chilena del Cobre—COCHILCO) has projected that copper production in Chile will increase over the next 9 years to reach 7.06 million tons in 2029 and peak at 7.25 million tons in 2025 [1]. However, an increase in copper production in deposits with an average grade of 1% or lower translates into a significant increase in tailings production, which is currently up to approximately 1.5 million t/day. A total of 757 tailings storage facility were identified in the last cadaster of mining operations in Chile [2]. Of all these deposits, 81.7% (606) correspond to classified sand tailings dams, of which 388 are inactive, 167 are abandoned and 51 are active. A total of 38 cases of physical instability have been reported and documented among the failures that have occurred in classified sand tailings dams between 1915 and 2010 in Chile. These cases

have been attributed to seismic liquefaction or flow failure (50%), slope instability with seismically induced deformations (32%) and overflow (18%). Some of these failures, such as those that occurred at the Barahona (1928), El Cobre (1965) and Las Palmas (2010) dams, have released tailings with catastrophic consequences in terms of the loss of human lives and environmental damage.

The main causes of physical instabilities in classified sand tailings dams in Chile were identified in [3], these causes corresponded to, the construction method, a poor cycloning process (fines content, FC > 20%), inefficient degree of compaction, a high degree of saturation and inappropriate embankment geometry (downstream slopes, the grade, freeboard and crest width). These causes have been directly related to poor construction/operation, inadequate deposit monitoring or a combination of these factors, where compaction control is among the key parameters affecting the physical stability of these types of deposits. The compaction control in classified tailings dam is commonly undertaken by measuring soil's in-situ unit weight ( $\gamma_t$ ) in a few points within the dam (technical specifications indicate minimum number of tests per volume or weight of compacted material). Depending on the operation, descriptive statistics is used to analyse the gathered data while spatial analysis of datasets is uncommon.

In [4] the relevance of carrying out compaction control considering both the variability in the physical characteristics of the sand tailings (e.g., mineralogy and particle size) and the variability resulting from the deposition, construction, and compaction of the embankment of classified sand tailings dam. A standard method was developed for the in-situ control of the degree of compaction with depth and the layer thickness of the sand tailings deposits using a PANDA penetrometer as a measuring instrument [5,6].

The method allows controlling economically, quickly, and efficiently, both the degree of compaction and the thickness of the deposited layer, considering both the material variability of the tailings sands, as well as the variability generated as a result of the construction process used. This tool generates in situ data more quickly over a larger depth range and in higher quantities than the sand-cone method, and nuclear densimeter, currently used in Chile to perform the compaction control of classified sand tailings dams [7]. Thus, the penetrometer is an effective tool for compaction control in sand tailings dams since it can cover a large surface area and deeper exploration depths in comparison to conventional superficial techniques (e.g., sand-cone method and nuclear densimeter). As part of the operational control of this type of facility, the use of these surface techniques implies carrying out a very small number of tests on the surface and reaching depths of less than 0.3 m, leaving questions about the state of compaction for more important depths. This information is not subsequently processed or spatialized, due to the compaction methodology applied for the construction of classified sand tailings dams, it is empirically validated by the same operators, without considering the optimization of the process.

The analysis of the generated compaction datasets can be performed using simple geostatistical techniques for spatial interpolation of a wide study area, considering a preferential distance and direction. This spatial estimation technique covers a large control surface for unsampled locations based on the location of field tests [8]. Thus, a geostatistical analysis can be used to model the spatial distributions of a study parameter over large areas, and the control volumes can be changed by switching to additive variables [9]. These methods have been used in geotechnics to develop spatial stratigraphic models and determine the index properties and geotechnical parameters, among other properties, of natural soil deposits, primarily using databases of surveys, standard penetration test (SPT), and cone penetration tests (CPT), e.g., [10–15].

Geostatistical techniques were used in the present study to develop spatial models of the  $\gamma_t$  and compaction degree for periodic compaction control in embankments of sand tailings dams based on the PANDA cone resistance ( $q_d$ ). First, variations in the physical characteristics, index properties and  $q_d$  were analyzed for classified sand tailings dams, which were considered representative of medium and large Chilean mining operations. The percentage of homogeneity or heterogeneity of each parameter was determined. Second,

geostatistics was applied to compaction control in an experimental classified sand tailings dam. A test area of the embankment was selected and compacted by the method typically used for the deposit. A geometric grid of survey points was defined for the study area within which 91 PANDA tests were performed down to a 1.5 m depth. The representativeness of the study area was assessed by performing a statistical analysis to comparatively analyze the means and variances of data from compaction control conducted over 3 years in the classified sand tailings dam and from field tests in the study area. The results of the Student's t-test and from Bartlett's test indicated the same means and variances for both datasets. The results for each control point were used to construct experimental vertical and horizontal semivariograms in different directions of analysis for  $q_d$ , the in situ dry unit weight ( $\gamma_d$ ) and the degree of compaction Standard Proctor ( $SP = 100 \times \frac{\gamma_d}{\gamma_{max}}$ , where  $\gamma_{max}$  corresponds to the maximum dry unit weight Standard Proctor test). These three parameters were best fit by a theoretical spherical semivariogram. After determining the spatial distribution of the three parameters, a stochastic interpolation method known as ordinary kriging (OK) was applied. The real and estimated  $q_d$  values were cross validated to compare the modeling results with the measured results for the survey grid and to validate the quality of the selected theoretical semivariogram model. From the results obtained, it is concluded that from the use of the Lightweight Penetrometer PANDA together with simple geostatistical techniques of spatial interpolation, it is feasible to perform quality control (QC) or quality assurance (QA) in a faster and more effective way compared to other techniques currently used (sand cone method [7], or nuclear density meter [16]). This speed and effectiveness were evaluated for classified sand tailings dams during construction. In this way, it is possible to more effectively identify SECTORS that do not comply with technical specifications defined as part of the facility design. Deviations from the design that can be identified using the geostatistical techniques in sand dams are: (i) zones of weak resistance and consequently with less degree of physical stability (e.g., greater potential for seismic liquefaction, a key aspect in countries with significant seismic activity, such as Chile [3,4]); (ii) over compacted areas, where the applied compaction process could be improved, optimizing the economic resources allocated for this purpose. (e.g., fewer machinery hours used for the compaction process).

## 2. Background

### 2.1. Compaction Control in a Classified Sand Tailings Dam

#### 2.1.1. Criteria

In Chile, a seismically active country, sand tailing dams must be mechanically compacted. The above is to ensure the dilative behavior of the sandy material upon shearing. Compaction results in material above the critical state line avoiding liquefaction risk and improving slope stability under seismic and monotonic loading [3,4,17,18].

Chilean engineering criteria (e.g., [3,17,19]) include the FC (<75  $\mu\text{m}$ ) of classified sand tailings used to build an embankment and the compaction degree among the key requirements for adequate physical stability (under static and seismic conditions) of tailings deposits during operational and subsequent closure stages. A FC range from 10 to 25% reconciles considerations of the material geotechnical properties (the densities, permeabilities and shear strength, among others) with the costs of the cycloning process. Compaction degree higher than 95% SP are deemed acceptable. Sand tailings with a FC between 10 and 25% and 95% SP have a relative density ( $D_r$ ) of 60 to 65% [18]. This  $D_r$  or SP is adopted in practice as a preliminary threshold, between contract (loose) and dilatant (dense) behavior of the sand tailings [20,21].

During the operational stage of the sand tailings dams, it must be checked periodically that the degree of compaction resulting from the applied compaction process complies with the value of SP or  $D_r$  established in the design project. This way, it ensures dilative behavior in the entire embankment and, therefore, a stable condition from the physical point of view [22–24].

Concerning the periodic monitoring of operational parameters in the sand tailings dams, the compaction control is carried out considering as a basis the requirements established by the National Service of Geology and Mining (SERNAGEOMIN, Ministry of Mining of Chile), together with the control criteria established internally by each mining company. SERNAGEOMIN requires mining companies to carry out a quarterly control through the official document called “Form E700” (<https://www.sernageomin.cl/formularios-seguridad-minera/> accessed on 5 November 2022). However, regarding compaction control, this control document has the following drawbacks:

1. It requests limited and punctual information (matrix with six control points for each quarter).
2. The E700 do not follow common control measures as to clearly characterise the in situ density and corresponding SP or Dr.
3. Reported Dr or SP values have some degree of uncertainty concerning the reference values used for compaction control.
4. The thickness of the compacted layer is not controlled.

For its part, current engineering practices use a limited number of reference samples (e.g., 3 to 5 control points are used for every 3000 m<sup>2</sup> or 50 m/L of the crest) and assume material homogeneity, albeit disregarding the thickness of the compacted layer.

Regarding the variability of deposited sand tailings, no standard methods are currently available in the country to control the degree of compaction efficiently, quickly, and economically, both on the surface and in-depth. Consequently, these factors and their effects on the actual mechanical behavior of this type of deposit remain unknown for noncontrolled areas due to limited checkpoints with limited space/time representativeness. The previous translates into uncertainties regarding the behavior of the tailings sands (contractive or dilative) and, consequently, the potential for liquefaction and slope instability of embankment.

### 2.1.2. Compaction Control Tests

The sand-cone method [7] and/or nuclear densimeter [16] are typically used to perform periodic compaction control of the sand layers deposited during the construction of an embankment of a classified sand tailings dam. However, the devices employed in these methods cannot be used to control the layer thickness. The test execution time of the sand-cone method limits the surface area that can be controlled. Ref. [4] addressed this issue by developing a method for compaction control in classified tailings dams in which the measuring instrument is a lightweight variable-energy dynamic penetrometer PANDA (Pénétromètre Autonome Numérique Dynamique Assisté par Ordinateur). The PANDA device is a 14-mm-wide rod with a metal cone at one end and a hammering head at the other end. The head is impacted by a standard 2-kg sledgehammer to drive the instrument into the soil (Figure 1). The cone area is 2 cm<sup>2</sup> in quality control (QC) mode and 4 cm<sup>2</sup> in quality assurance (QA) mode. The maximum penetration depths in QC and QA modes are 1.5 m and 6 m, respectively, in soils with a maximum size below 50 mm.

The impact of the hammer generates a stress wave in the hammering head that propagates towards the tip to drive the rod into the soil. The penetration ( $e$ , mm) and the cone resistance ( $q_d$ , MPa) for each blow are continuously recorded using the Dutch formula [25–28], assuming a perfectly inelastic impact between the hammer and the hammering head and neglecting the penetrometer and soil deformation.

The assumptions of the Dutch formula can be met during a PANDA test by controlling the driving energy to ensure that the penetration from a hammer blow ranges from 2 to 20 mm [29,30]. An almost continuous record of  $q_d$  v/s  $e$  is obtained. Therefore, the layer thickness can be estimated, and compaction problems can be identified.

During the PANDA test, a microprocessor receives a signal generated by the sensor in the cone and automatically records  $q_d$  and  $e$  for each hammer blow. The in-situ background noise of the penetrogram is eliminated by applying a signal filter for signal smoothing or regularization with a fixed 25 mm wide moving window. The penetrometer signal is compared with a preset control curve (e.g., [27,29,30]) in compaction control mode

based on prior soil classification, by the American Association of State Highway and Transportation Officials (AASHTO) or the United States Geological Survey (USGS) systems, and given the compaction level and the moisture content (dry, medium, and wet) for the compaction process. As a reconnaissance tool in tailings deposits, the results obtained from the PANDA test have the following applications: estimation of geotechnical parameters in-depth, operational control of thickened tailings deposits, estimation of liquefaction potential (e.g., [27,29,30]).

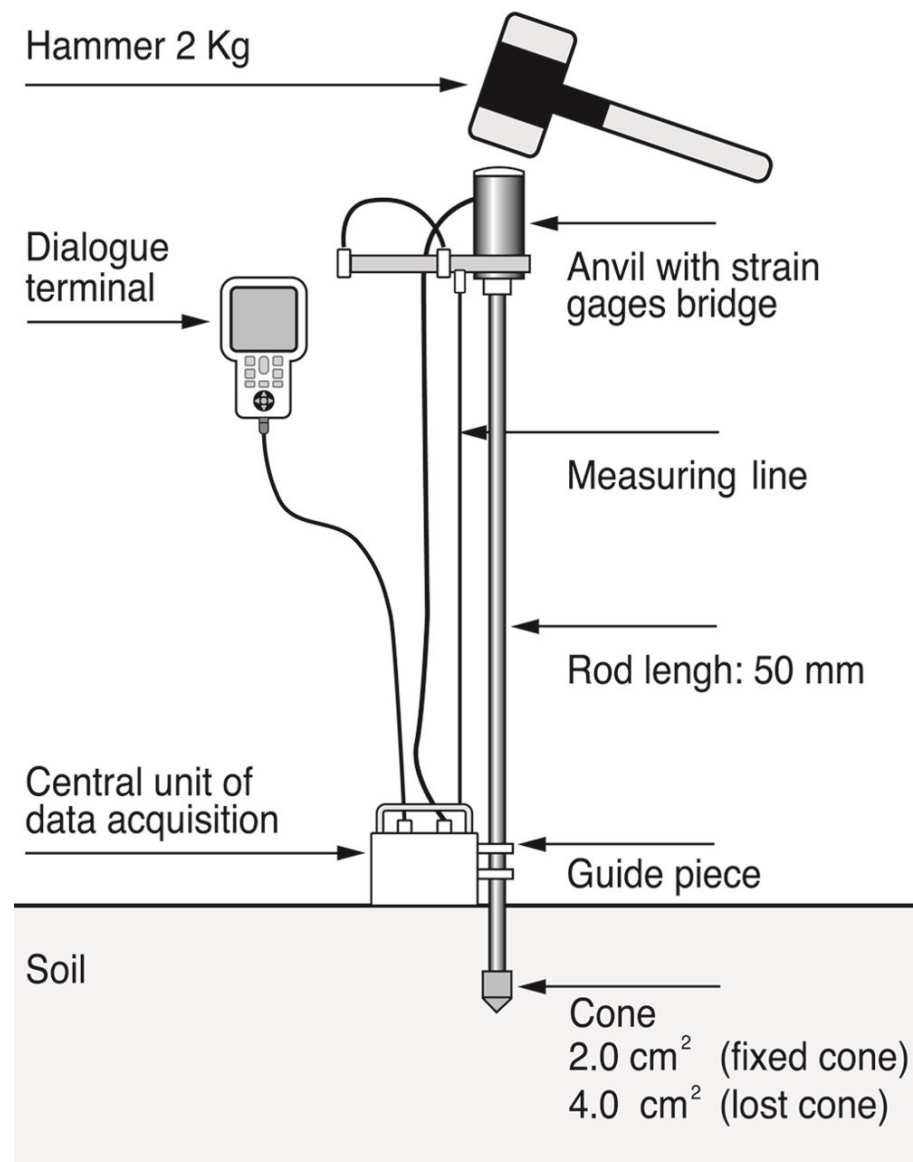


**Figure 1.** PANDA lightweight penetrometer scheme [18].

The existing correlation between  $q_d$  and  $\gamma_d$  of the soil depends on the nature and the water content ( $w_{nat}$ ) of the material to be controlled. It is based on hypotheses derived from the micromechanics of granular media, which postulate that the characterization of the mechanical behavior of a material is carried out from the description of its microstructure [31], considering three families of data: nature of the grain, the interaction between two grains and fluids, set of grains. Based on this hypothesis, according to a micromechanical logic and within a geotechnical context [32,33] proposed the following classification: natural parameters (mineralogy, particle size distribution, and grain shape), natural parameters of the set of particles ( $\gamma_d$  or void ratio) and interaction parameters ( $w$  and Atterberg limits).

This translates into a particular mechanical response for a type of soil. In this way, if the parameter to be measured in-situ is  $q_d$ , under the assumption of reversibility (unbreakable grains, resistance to wear, and suction reversibility) and knowing the nature and interaction parameters, it is possible to determine in-situ  $\gamma_d$  of the material.

The works carried out in [34,35], experimentally and analytically demonstrated (cavity expansion theory), that in granular soils it is possible to estimate  $\gamma_d$  from the point resistance (e.g.,  $q_d$ ) obtained from penetration tests. Although this function would not meet the limit conditions, regarding the state of minimum and maximum compactness, it is valid for the range of density that would have to be controlled in-situ (e.g., 95% SP in classified sand tailings).

## 2.2. Variability in the Geotechnical Properties of Sand Tailings

An extensive study on the variation in geotechnical properties of sand tailings is not available in the literature. A few studies have been conducted to establish the ranges of values selected index or shear strength properties (e.g., [36–39]). In [40] it was identified potential sources of variability in the physical and mechanical characteristics of the sand tailings. These sources were classified into 4 levels: These sources were classified into four levels: (i) level 1: Production size (mining scale); (ii) level 2: tailing manufacturing: crushing, pressing and flotation; (iii) level 3: deposition: cyclone, construction and compaction method (e.g., simple hydraulic deposition and mechanical compaction layer-by-layer); (iv) level 4: deposit age: aging effects, under progressive drying conditions over time. Two types of variability were identified: material, which is associated with the intrinsic properties of the tailings (e.g., mineralogy, particle size distribution and plasticity of the fraction of fines smaller than 75  $\mu\text{m}$ ), and structural, which is associated with the construction process used (e.g.,  $\gamma_d$  and layer thickness). Figure 2 shows the variability of the particle size distribution (PSD) obtained as part of the operational control carried out in the embankment of sand tailings dams of medium copper mining in Chile. The embankment of a classified sand tailings dams exhibits both temporal and spatial variability. Temporal variability depends on material aging induced by physicochemical bonding between particles, gradual drying and changes in stress states, among others [20,41]. Table 1 presents a group of factors that generate material and structural variability in sand tailings on both spatial and temporal scales. Another factor to consider, which contributes to the variability of the  $q_d$  values, corresponds to the prospecting depth reached in the embankment, particularly if it is required to carry out a quality assurance using penetrometers (e.g., SPT, CPTu, Lightweight Penetrometer PANDA, among others), for depths greater than 1.5 (m) For shallower depths, the influence of depth is not considered on the values of  $q_d$ , within the context of compaction control [29]. Within this context [28], analyzed the effects of soil conditions (dry unit weight, overburden stress and water content of the surrounding soil, and fine content) on the cone resistance ( $q_d$ ) of lightweight penetrometers (PANDA), from a series of tests in a calibration chamber. An overburden correction factor ( $C_N$ ) for sand tailings was obtained as part of the results. This factor allows considering the influence of depth on the measurements of  $q_d$ .

**Table 1.** Types of variability, associated factors, effects, and variation in geotechnical properties sand tailings.

Level	Factor	Variability		Effects	Variation in Geotechnical Properties
		Type	Scale		
1	Production size (mining scale)	Material	Spatial	Degree of homogeneity or heterogeneity of whole tailings in terms of constituent residual minerals (mineralogical species and grade of the field of origin)	Particle size distribution (PSD) and specific gravity of solid particles (G)
2	Crushing, pressing and flotation	Material		Physical characteristics and incorporation of chemical reagents into whole tailings	
3	Deposition: cycloning, construction and operation method	Material and structural		Physical characteristics and geotechnical properties of sand tailings	PSD of sand tailings, in-situ dry unit weight and water content, shear strength parameters
4	Deposit age	Material	Temporal	Aging of sand tailings: generation of cohesion by case-hardening	Gradual increase in geotechnical properties and rigidity

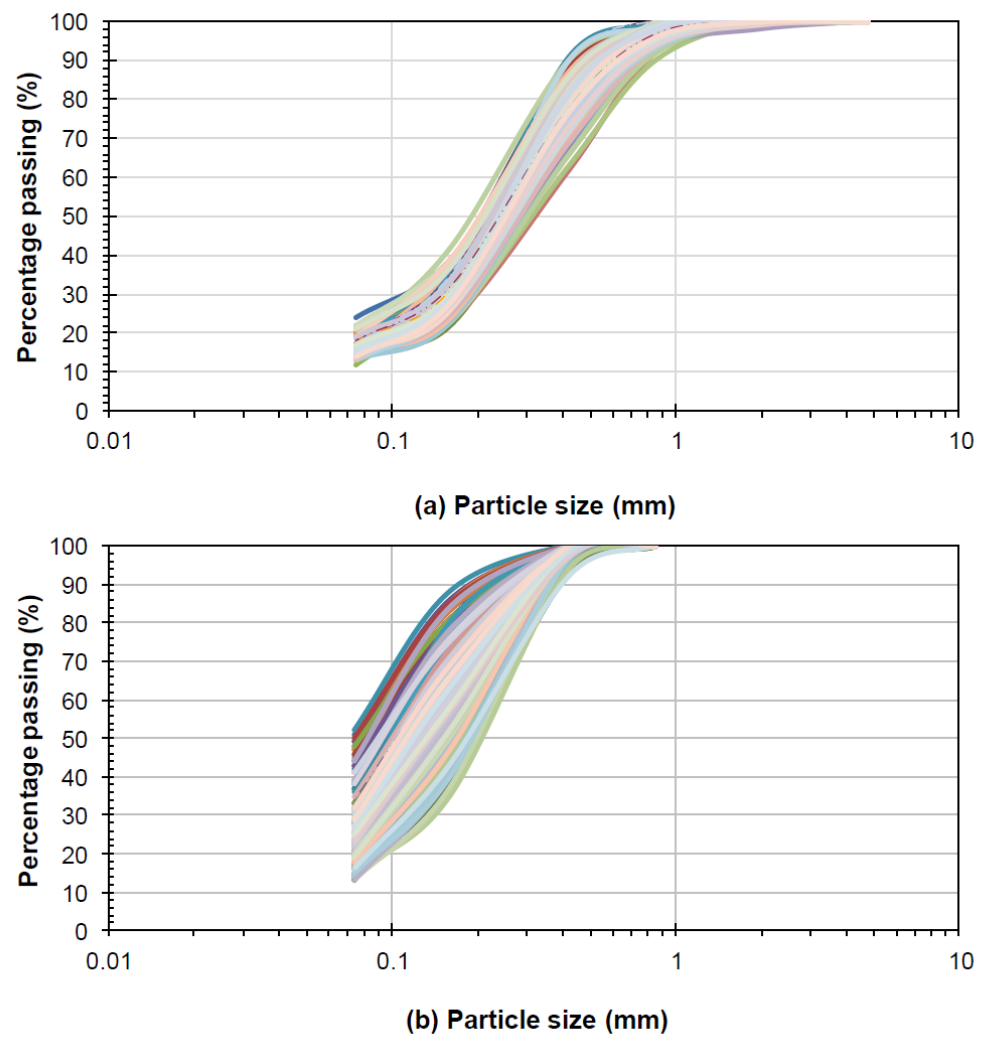


**Figure 2.** Variation of the particle size distribution (PSD). Operational control of two sand tailings dams of medium copper mining in Chile. (a) Sand tailings T1. (b) Sand tailings T2. (see Table 2).

**Table 2.** The construction method and technical specifications defined in the design project of different tailings dams of medium and large Chilean copper mining companies.

Sand Tailings Dam	Type	DS Slope V/H	Height m	Production of Sand Tailings	Construction of the DS Slope		
					Deposition and Distribution of Sand Tailings	Compaction	Specified Degree of Compaction
T1	DS and CL	1:3.5	30	Cycloned sand tailings derived from various deposits	From cyclones (underflow) in the crest of the deposit and levelling with a bulldozer	DS slope and crest in 50–60-cm layers in the direction of the slope by a 20-t bulldozer	95% SP
T2	CL	1:2.7	20			Crest in 20–40-cm layers in the horizontal direction by a 300-kg vibratory plate compactor	
T3	CL	1:3.5	60	Cycloned sand tailings derived from a single deposit		DS slope and crest in 30–40-cm layers in the slope direction by a 20-t vibratory roller	
T4	DS	1:2.5	40			DS slope and crest in 30–40-cm layers in the slope direction by an 18-t bulldozer	
T5	DS	1:2.5	40		From dump trucks and distribution with a bulldozer	DS slope and crest in 30–40-cm layers in the horizontal direction by a 20-t vibratory roller	95% Modified Proctor (MP)

Table 2. Cont.

Sand Tailings Dam	Type	DS Slope V/H	Height m	Production of Sand Tailings	Construction of the DS Slope		
					Deposition and Distribution of Sand Tailings	Compaction	Specified Degree of Compaction
T6	DS	1:3.0	150		From cyclones (underflow) in the crest of the deposit and leveling with a bulldozer	DS slope and crest in 50-cm layers in the slope direction by a 10-t vibratory roller	95% SP

### 3. Materials and Methods

#### 3.1. Variation in $q_d$ for Sand Tailings Dams

As an illustration, data from various PANDA experiments were collected and analyzed to show the variation in  $q_d$  for various classed sand tailings dams (Figure 3). The PANDA tests were performed for compaction control during the operation phase of six deposits located in Chile. The range of embankment heights from 20 to 150 m is representative of medium and large Chilean mining operations (Table 2).

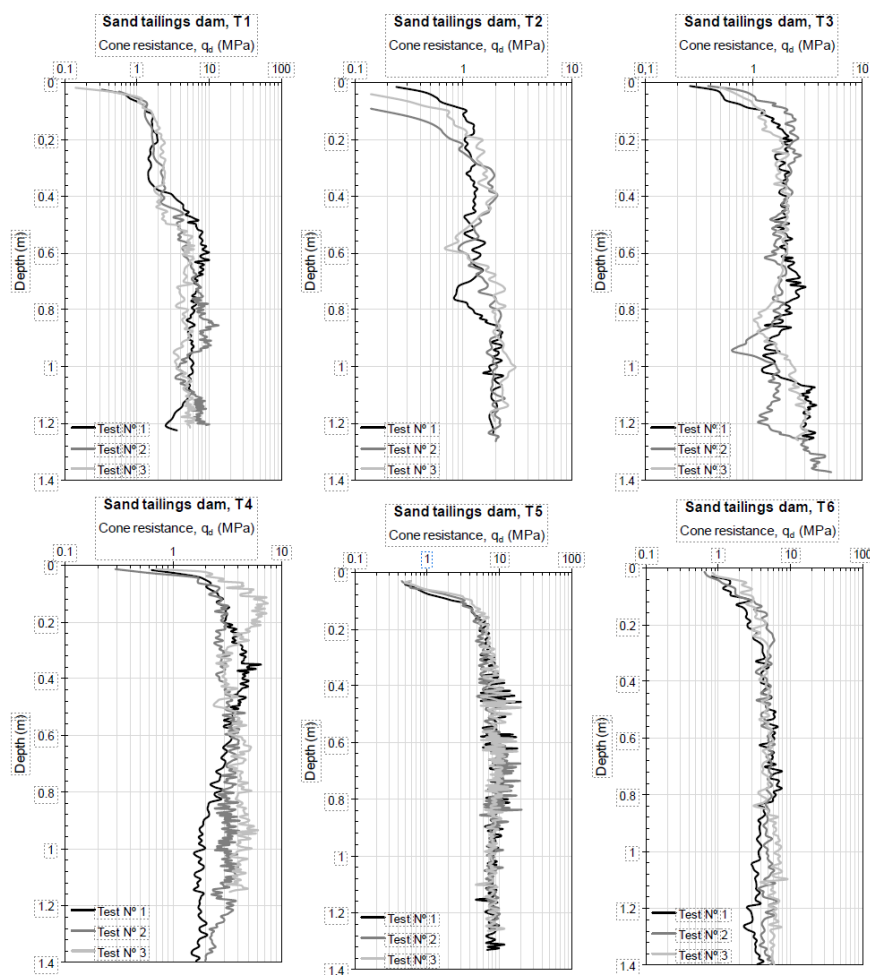


**Figure 3.** Cone resistance ( $q_d$ ) as a function of depth, measured in 6 Chilean classified sand tailings dams.

The variation in  $q_d$  among classified sand tailings dams is directly associated with the physical characteristics (the particle size distribution and density of solid particles),  $w_{op}$ , %SP, and layer thickness of sand tailings and the compaction method. The  $q_d$  values increased and became more homogeneous with depth in deposits that were systematically and mechanically compacted with vibratory roller.

The results for six classified sand tailings dams (Table 3) were statistically analyzed using the criteria of homogeneity or global heterogeneity defined by [42] as a function of the coefficient of variation (CV%). The embankment materials were consequently classified as nonplastic silty sands (SM). The specific gravity (G) of the sand tailings was homogeneous across different deposits. The FC varies among sand tailings from different fields, and the resulting mean heterogeneity is associated with changes in the production process that affect the mineralogical species and the grade of the extracted mineral.

**Table 3.** Geotechnical properties of mine tailings based on statistical analyses of experimental data from Control compaction or quality control (QC) for six Chilean sand tailings dams.

Geotech. Prop.	Dataset: Operational Control in Sand Tailings Dams																							
	T1 <sup>a</sup>				T2 <sup>a</sup>				T3 <sup>a</sup>				T4				T5				T6			
	Data	Av.	CV %	Var. Class	Data	Av.	CV %	Var. Class	Data	Av.	CV %	Var. Class	Data	Av.	CV %	Var. Class	Data	Var.	CV %	Var. Class	Data	Var.	CV %	Var. Class
G	108	3.09	4.6	Homo.	45	3.36	8	Homo.	40	3.07	2.2	Homo.		3.07	2.2		161	2.7	1.5		19	2.69	0.9	Homo.
$D_{50}$ [mm]		0.13	19.0	Homo.	262 <sup>b</sup>	0.11	15.2	Homo.		0.25	8.7	Homo.	40	0.17	17.3			0.3	7.8			0.32	32.2	Medium hetero.
FC [%]	3266	28	28.7	Medium hetero.	262 <sup>b</sup>	33	26.3	Hetero. media	2958	17	10			27	19.4		1206	13	18.3		44	16	8.7	
$\gamma_{dmax}$ [kN/m <sup>3</sup> ]		18.2	6.2		262 <sup>b</sup>	20.8	8			18.5	2.3			18.2	5.1			18.2	5.1			16.7	1.0	
$\omega_{op}$ [%]	392 <sup>b</sup>	15.2	9.4		262 <sup>b</sup>	14.4	10.3	Homo	495 <sup>b</sup>	14.3	6.2	Homo	8	15.6	5.5	Homo	17 <sup>b</sup>	11.1	14.5	Homo	23 <sup>c</sup>	17.8	3.9	Homo.
$\gamma_d$ [kN/m <sup>3</sup> ]		17.5	6.6	Homo	275 <sup>b</sup>	20.1	8.2			18.1	2.9			19.1	2.3			17.4	3.0			16.0	1.1	
$\omega_{nat}$ [%]	3266	11	22.3		275 <sup>b</sup>	3.3	43.1	Hetero. media	2958	7.5	27.3	Medium hetero.	79	6.1	18.7		79	8.6	15.5		356	12.7	15.2	
$\gamma_t$ [kN/m <sup>3</sup> ]		19.4	6.7		275 <sup>b</sup>	20.7	8.2	Homo.		19.5	3.5	Homo.		20.3	2.6			18.8	2.5			18.1	2.2	
$q_d$ [MPa]	275	4.8	50.6	Highly hetero.	75	2.87	45.9	Highly hetero.	100	1.95	52.8	Highly hetero.	75	2.71	42.4	Highly hetero.	20	6.48	48.6	Highly hetero.	15	7.04	31.4	Medium hetero.

Note: Av: Average, CV %: coefficient of variation,  $D_{50}$ : median grain size, <sup>a</sup> Database from [30], <sup>b</sup> Standar Proctor test, <sup>c</sup> Modified Proctor Test.

The  $\gamma_{dmax}$ , and  $w_{op}$  values are case-dependent and vary with the mineralogical species, grade of the field of origin and production process. However, these parameters are homogeneous for the same deposit. In turn, the  $\gamma_t$  and  $\gamma_d$  can be controlled for the individual compacted layers from the surface and are classified as homogeneous for a single deposit. The  $w_{nat}$  can vary from medium heterogeneous to homogeneous, primarily depending on the time and climatic conditions (temperature and relative humidity) under which the test is performed. All classified sand tailings dams exhibit a highly heterogeneous variation in  $q_d$  with depth that is mainly generated by the multilayer structure created by the embankment construction process (deposition, distribution and compaction). Ref. [40] have reported that the index properties of the sand tailings can be described by a normal distribution, whereas  $q_d$  follows a log-normal distribution. Thus, the variability of sand tailings can be considered well defined and determined given the nature of the deposited materials and the structure resulting from the construction process.

The spatial structural variability in the embankment of a sand tailings dam is reflected in the variation in  $q_d$  at the surface and with depth. This variation reflects two key factors: the state of the structure between strata and the variability inherent to the compaction process (the machinery efficiency and compaction energy homogeneity). The variation in  $q_d$  also reflects changes in the  $w_{nat}$ , which is associated with the temporal variability of these materials.

The simplicity, speed and accuracy of the PANDA test facilitates the reconstruction of the multilayer structure along the depth of classified sand tailings dams during the construction phase. Correlating  $q_d$  with other geotechnical parameters, (e.g., the friction angle, compactness state and cyclical resistance) can be used to identify areas of low resistance and facilitate the assessment of the actual physical stability at different points of the structure and at any time during operation. Thus, the utility of geostatistics tools for the characterization and modeling of the spatial structure generated during operation of a sand tailings dam emerges within the context of routine compaction control.

### 3.2. Geostatistical Analysis for the Characterization of Structural Variability in a Classified Sand Tailings Dam

Geostatistics is generally applied to structural geotechnical data in the following stages [43]: (i) an exploratory database analysis is performed to determine basic statistical parameters (the mean, standard deviation, coefficient of variation and maximum and minimum values), identify outliers and calculate the data distribution; (ii) a structural data analysis is performed to determine the vertical and horizontal correlation distances that can be fitted by a theoretical semivariogram (spherical, exponential, Gaussian, cubic and linear, among others); (iii) estimation and simulation based on spatial correlation data and a theoretical model are performed to estimate (virtual) profiles of the geotechnical properties of interest and (iv) a 2-or 3-dimensional map is constructed to facilitate the interpretation of the numerical estimation and simulation results.

An experimental semivariogram (1) is defined as the semiaverage of the square differences between of all pairs of observations separated by a distance  $h$  (e.g., [44–48]).

$$\gamma(h) = \frac{1}{2N(h)} \sum_{i=1}^N [Z(x_i) - Z(x_i + h)]^2 \quad (1)$$

In the (1),  $\gamma(h)$  is the semivariance estimated for a distance  $h$ ;  $N(h)$  is the number of pairs of observations separated by a distance  $h$ ;  $Z(x_i)$  is the value of the random variable at a point and  $x_i$  and  $Z(x_i + h)$  is the value of the random variable at a distance  $h$  from point  $x_i$ .

A semivariogram model is only stationary if a Random Function is stationary, the variogram model must be of stationary type [8]. In [15] the authors have proposed that most soil science or geological engineering data are homogeneous and meet at least the criterion of weak stationarity.

After identifying and modeling the spatial structure of the observations, the Kriging stochastic interpolation procedure is applied [46]. The Kriging estimates a regionalized variable ( $q_d$  and the % SP) at a site without information through a linear combination of the information available from sampled sites. Each observed value is weighted based on the structure of the regionalized phenomenon (given by the variogram) and the geometric characteristics of the sampling (values and location), subject to a universal quantification procedure, as indicated in (2) and (3).

$$Z_v^* = \sum_{i=1}^n \lambda_i Z(x_i) \quad (2)$$

$$\sum_{i=1}^n \lambda_i = 1 \quad (3)$$

This methodology has been widely used to interpolate cartographic data. The main advantage of this methodology against classical interpolation methods (e.g., inverse distance weighting (IWD) is the determination of the minimum estimation error, given by the Kriging variance. The estimation variance is minimized to ensure the optimal use of the available information (e.g., [10,44,49,50]). The Stanford Geostatistical Modeling Software (SGeMS) was used as a calculation tool in the present study.

### 3.3. Classified Sand Tailings Dam under Study

The classified sand tailings dam investigated in this study is located at northern of Chile and stores waste generated from the flotation processing of copper sulfides from a single field. Therefore, the physical characteristics and mineralogical characteristics of the generated tailings can be considered homogeneous.

This deposit called T3 in the present study began operating at the beginning of the 21st century, storing 50 million tons of tailings. The dam was constructed using the CL method from a starter embankment built with loan material. The tailings are classified by placing hydrocyclones on the crest of the embankment. The classified sand tailings have deposition  $w_{nat}$  levels ranging from 28 to 30%. Subsequently, these tailings sands are distributed and compacted using the following methodology: (i) distribution and profiling of the tailings sands cycloned by a bulldozer after having obtained the optimum moisture content  $w_{op}$  Standard Proctor test until reaching the necessary layer thickness considering the percentage of swelling that it experiences the material. (ii) once the optimum humidity for compaction has been reached, compaction is carried out in layers of thickness equal to 0.4 m. on average, by round-trip cycles of a vibrating smooth roller of 20 t of static weight, carried out in the longitudinal direction of the slope. (iii) finally, a bulldozer pass is applied in order to roughen the surface of the deposited layer and thus mitigate the effects of wind erosion. The compaction control parameters defined in the design project are the following: FC = 12%,  $\gamma_{dmax} = 19.87 \text{ kN/m}^3$ ,  $w_{op} = 16.3\%$  and % SP = 95%.

#### Field Study and Survey Grid

A field study of the classified sand tailings dam was performed in a 120-m-wide by 45-m-long study area of the DS of the recently compacted embankment, which was overlaid with a survey grid (Figure 4). The regionalized variable analyzed in this study was  $q_d$ , which was assessed as a function at different depths in each observation point. Note - the variable is a regionalised function of the field coordinates  $q_d(x, y, z)$ .

The grid was divided into 4 slabs on which 91 PANDA tests were performed in control compaction mode or quality control (QC) up to a depth of approximately 1.5 m. The grid points were arranged 7 m apart in the DS direction and 10 m apart in the direction parallel to the embankment crest. The regionalized variable analyzed in this study was  $q_d$ , which was assessed as a function of the 3D field coordinates point.

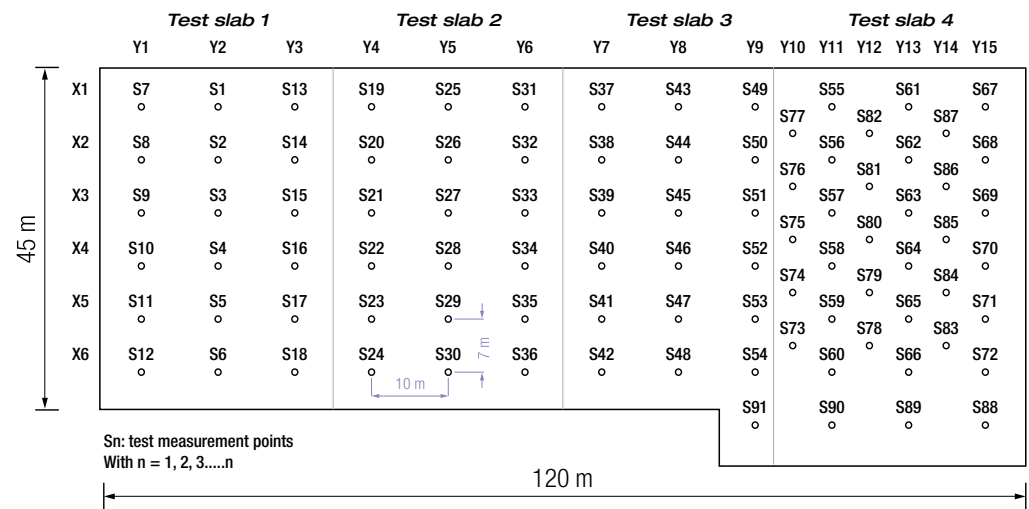


Figure 4. Geometry of the survey grid and PANDA test points. DS slope embankment of classified sand tailings dam T3.

#### 4. Results and Discussion

This section has objective describes and analyzes the results. As a starting point,  $q_d$  is statistically analyzed. Subsequently, semivariograms are used to finally use ordinary kriging in order to model  $q_d$ , and estimate  $\gamma_d$  and % SP.

##### 4.1. Physical Characteristics and Compaction Parameters of Classified Sand Tailings in the Study Area

The representativeness of the study area selected in the embankment classified sand tailings dams were assessed in terms of the physical characteristics and compaction parameters of the deposited sand tailings. Thus, a descriptive statistical analysis was carried out on data from compaction controls performed over the preceding 3 years and data collected in the area of the embankment with the survey grid (Table 4).

A preliminary analysis of the results shows that the study area is representative of the entire embankment in terms of the particle size distribution or PSD (FC and  $D_{50}$ ),  $\gamma_{dmax}$ ,  $\omega_{op}$ , and  $\gamma_d$  of the classified sand tailings used to build the embankment. These results reflect material and structural (layer-by-layer) spatial homogeneity, which is primarily related to an invariant and well-controlled production process (pressing, flotation and cycloning) and a suitable construction and compaction method. The  $w_{nat}$  levels exhibit medium heterogeneity because this parameter depends on the time of and ambient temperatures during in situ sampling.

The representativeness of the study area with the survey grid was assessed using the Student’s t-test and Bartlett’s test to statistically analyze differences between means and variances at global and local scales. The same means and variances are found for each parameter (Tables 5 and 6).

**Table 4.** Summary of statistics for the total sample and the study area for the embankment and classified sand tailings dam T3.

Statistical Parameter	FC [%]		$D_{50}$ [mm]		$\gamma_{dmax}$ [kN/m <sup>3</sup> ]		$\omega_{op}$ [%]		$\gamma_d$ [kN/m <sup>3</sup> ]		$\omega_{nat}$ [%]	
	M A	M B	M A	M B	M A	M B	M A	M B	M A	M B	M A	M B
Sample	M A	M B	M A	M B	M A	M B	M A	M B	M A	M B	M A	M B
Data	3266	178	3266	178	495	35	495	35	3266	202	3266	202
Minimum Value	11	14	0.25	0.2	17.4	18.1	12.0	13.5	16.4	16.9	2.3	4.0
Maximum Value	24	21	0.46	0.28	19.8	19.5	16.3	16	19.8	19.8	19	14.3
Media	17	17	0.25	0.24	18.5	18.8	14.3	18.7	18.1	18.5	7.5	8.7
$\sigma$	1.7	1.5	0.022	0.016	0.43	0.36	0.89	0.98	0.52	0.61	2.05	2.68
CV%	10	8.9	8.7	6.6	2.3	1.9	6.2	5.2	2.9	3.3	27.3	30.8

Note: M A: total sample, M B: grid sector sample,  $\sigma$ : standard deviation.

**Table 5.** Results from the test of equality of means at global and local scales. Confidence level: 99.9%.

Parameter	Level	Data	Average	Student's <i>t</i> -Test Value	Confidence Interval $\Delta$ Means	Equality of Means
FC [%]	Global	3266	17	−2.8984	[−0.784, 0.049]	Yes
	Local	178	17			
$D_{50}$ [mm]	Global	3266	0.25	6.507	[0, 0.018]	Yes
	Local	495	0.24			
$\gamma_{dmax}$ [kN/m <sup>3</sup> ]	Global	495	18.5	−3.7449	[−0.053, 0.013]	Yes
	Local	35	18.8			
$\gamma_d$ [kN/m <sup>3</sup> ]	Global	3266	18.1	−9.4948	[−0.532, 0.012]	Yes
	Local	178	18.5			

**Table 6.** Results from the test of equality of variances at global and local scales. Confidence level: 99.9%.

Parameter	Level	Data	Variance $\sigma^2$	Coefficient Between $\sigma^2$	$\sigma^2$ Variation	Equality of Variances
FC [%]	Global	3266	2.721	1.01	[0.755, 1.526]	Yes
	Local	178	2.474			
$D_{50}$ [mm]	Global	3266	0.00048	1.92	[1.286, 2.661]	Yes
	Local	495	0.00025			
$\gamma_{dmax}$ [kN/m <sup>3</sup> ]	Global	495	0.190	1.52	[0.579, 1.037]	Yes
	Local	35	0.125			
$\gamma_d$ [kN/m <sup>3</sup> ]	Global	3266	0.281	0.76	[0.536, 1.037]	Yes
	Local	178	0.368			

#### 4.2. Statistical Analysis of $q_d$

The geostatistical evaluation was performed in the following stages: (i) a descriptive statistical analysis is performed of the PANDA penetrometers recorded collected in the study area and at the local level for each test slab; (ii) experimental variograms are calculated in different directions (at global and local levels); (iii) a theoretical variogram model is fitted to the experimental variogram and iv) the OK technique is used to estimate the study variables ( $q_d$  and the % SP) [46]. An analysis of the frequency histograms shows that the  $q_d$  values assessed at the global level of the survey grid and for each test plan follow the typical distribution of the penetrometers recorded for the classified sand tailings dams (Figure 5). The assumption that the  $q_d$  values follow a log-normal distribution is thus verified (e.g., [51,52]). The  $q_d$  v/s e penetrometers were smoothed using a 2.5 cm moving average to remove background noise from the signal recorded in-situ from each trial PANDA performed on the survey grid. The statistical analysis of the  $q_d$  values is presented in Table 7.

A maximum value of 8 MPa was identified from the statistical analysis results for the smoothed variable  $q_d$ . The  $q_d$  values assessed above this threshold (0.88% sample) for the case under study would correspond to overcompaction near a 100% SP and some case-hardening resulting from the progressive drying that sand tailings are subjected to, particularly in northern Chilean deposits.

**Table 7.** Statistical summary of in-situ  $q_d$  measurements for the full survey grid and test slabs.

Sector	PANDA Tests	No. of Pairs [ $q_d$ (MPa), $z$ (cm)]	Minimum and Maximum Values	Average	$\sigma$	CV%
Full grid	91	18,806	0.1 and 29.5	2.79	1.74	62.4
Slab N° 1	18	3850	0.14 and 22.7	2.96	1.88	63.5
Slab N° 2	18	4218	0.15 and 9.4	3.17	1.55	48.9
Slab N° 3	19	3728	0.19 and 29.5	3.24	1.96	60.5
Slab N° 4	36	7010	0.1 and 9.34	2.22	1.48	66.7

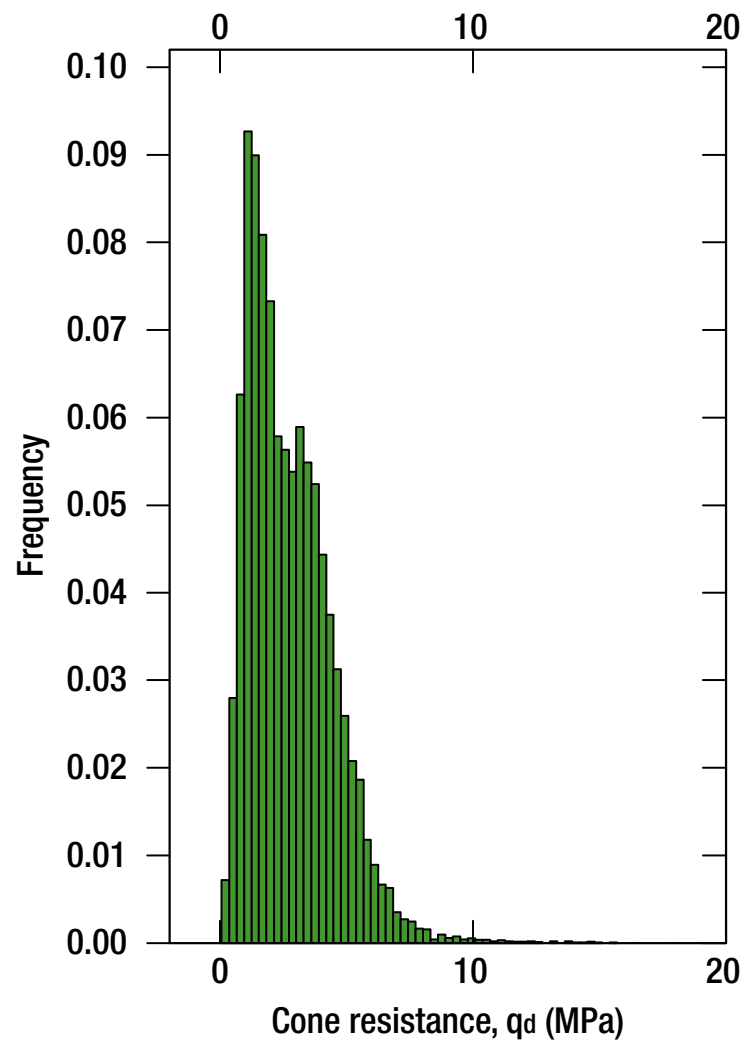


Figure 5. Histogram of  $q_d$  values. Full survey grid.

### 4.3. Experimental and Theoretical Semivariograms

#### 4.3.1. Calculation Parameters

Calculation parameters were defined to obtain the experimental semivariograms of the survey grid both globally and for the test slab (Table 8). The anisotropy of the study area was analyzed considering different azimuth values in the xy-plane and in vertical direction (the z-axis). “Lag separation” values were defined considering the geometry of the survey grid and the PANDA test results, smoothed every 2.5 cm.

Table 8. Parameters of the experimental semivariograms of  $q_d$  at a global level using the survey grid and the local level using test slabs.

Scale	Direction of Analysis	Semivariogram Calculation Parameters					
		Lag Separation [m]	Lag Tolerance [m]	Azimuth [°]	Tolerance [°]	Dip [°]	Bandwidth [°]
Survey grid	Horizontal x-y	7	3.5	0, 45, 90, 135	22.5, 90	0	5
	Vertical z	0.025	0.0125	0	22.5	90	3
Test slabs	Horizontal x-y	7	3.5	0, 45, 90, 135	22.5, 90	0	5
	Vertical z	0.0125	0.0125	0	22.5	90	3

#### 4.3.2. Semivariogram Modeling

##### - Results obtained in the vertical direction

In the vertical direction, the 2.5 cm “lag separation” defined for the  $q_d$  values produces a virtually continuous experimental semivariogram that facilitates fitting the theoretical model for the full survey grid and each test slab. A Different spherical models are found to fit all the experimental results (Figures 6 and 7). This type of model reasonably accommodates strata or layered structures and is therefore widely used in several fields of geoscience (e.g., [13,46,53,54]).

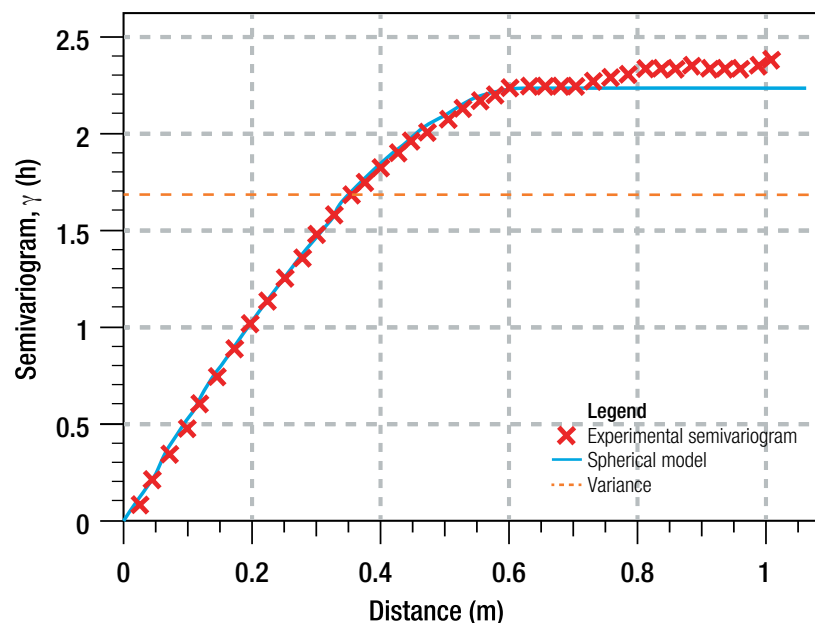


**Figure 6.** Experimental semivariogram and omnidirectional theoretical model for  $q_d$  in the vertical direction. Full survey grid.

Well-defined sills and ranges (Table 9) reflect the multilayer structure produced by the construction and compaction process. The range is approximately between 0.4 and 0.7 m and represents the global variability in the layer thickness. In turn, the increase in the experimental semivariogram values, put in evidence a different behaviour of the local variograms (in the different test slabs): quasi-stationary up to 0.4–0.6 m and not stationary or periodic for larger distances. A periodic behaviour of the experimental variogram reflects similar  $q_d$  values at distances approximately twice the theoretical range, especially for test slabs 1 and 2 [46]. The higher experimental semivariogram values for test slab 3 reflect a layered structure in which  $q_d$  gradually increases with depth. Note that test slab 4 does not have a well-defined sill over a range of approximately 1.2 m, which is near the maximum survey depth of 1.5 m reached in the PANDA tests. Consequently, the multilayer structure cannot be clearly identified for this specific area. This result may be associated with deviations in the method usually used to build the embankment, especially because the deposited layers were considerably thicker than those specified in the project (theoretical thickness: 0.5 m).

##### - Results obtained in the horizontal direction

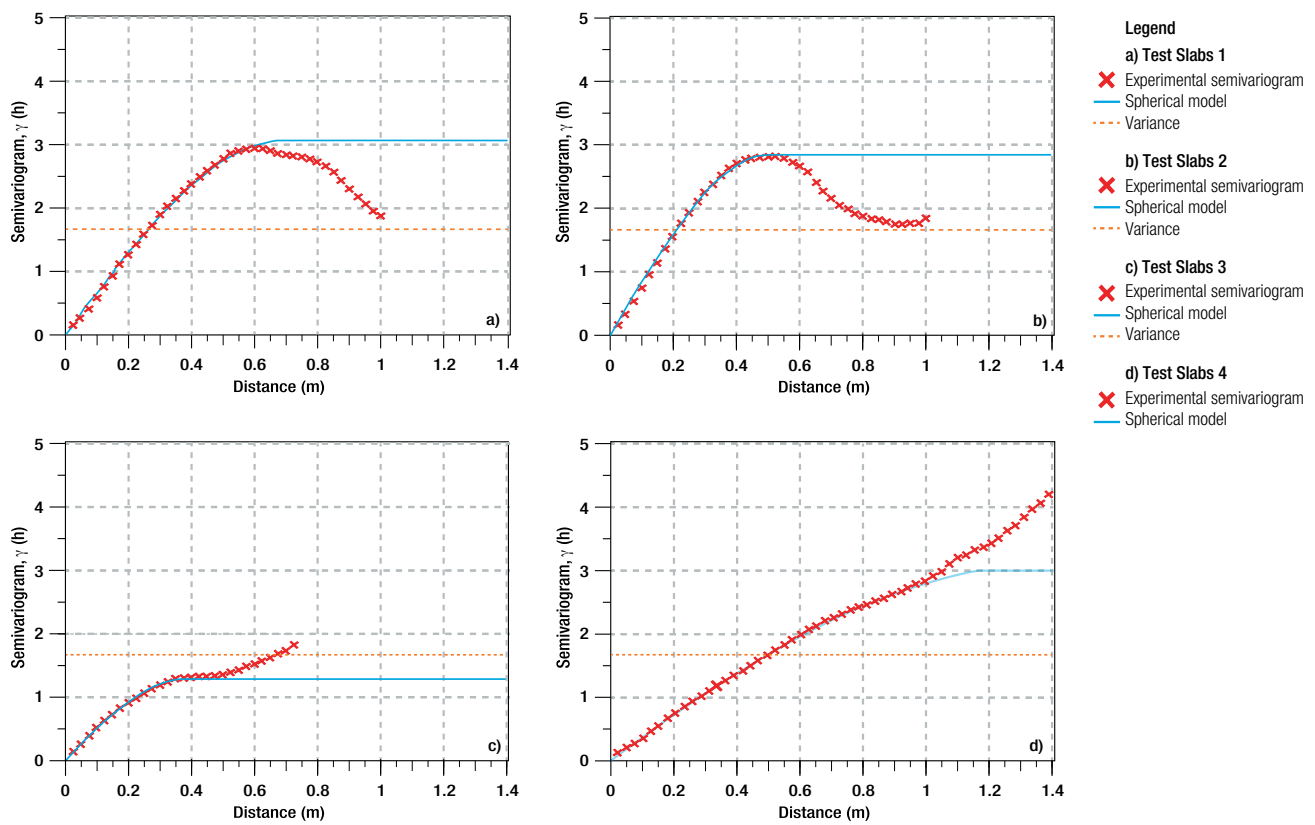


Figure 7. Experimental semivariograms and theoretical models for  $q_d$ . Vertical analysis plane.

Table 9. Experimental results for vertical and horizontal semivariograms of  $q_d$  based on the full survey grid and test slabs.

Scale	Plane of Analysis	Estimate Semivariogram					
		Azimuth/Inc [°]	Structure	Model	Nugget, $C_0$ [MPa] <sup>2</sup>	Sill $C_0 + C$ [MPa] <sup>2</sup>	Range [m]
Survey grid	Vertical z	0°/−90°	Single	Spherical	0	2.23	0.6
		0°/0°		Spherical 1	0	1.67	8.9
			Spherical 2	0	0.38	39.9	
	Horizontal x-y	45°/0°	Double	Spherical 1	0	1.62	8.6
				Spherical 2	0	0.40	36.1
		Spherical 1		0	1.61	8.2	
		Spherical 2		0	0.40	35.1	
		90°/0°		Spherical 1	0	1.62	7.9
Spherical 2				0	0.42	33.7	
Test Slab	Vertical z	0°/−90°	Single	Spherical	0	3.08	0.7
					0	2.85	0.5
					0	1.21	0.4
					0	2.98	1.2

A theoretical semivariogram model in the horizontal plane of the embankment was designed at the level of the full survey grid by analyzing the experimental semivariograms in different directions or azimuths (Table 9). Experimental semivariograms in the horizontal direction could not be generated for the test slab because of an insufficient number of points in the xy-plane. The semivariograms for the full survey grid exhibited some anisotropy in the xy-plane to the downstream talus of the retaining dyke (Figure 8). The best fit in the horizontal direction was obtained using two nested spherical models [55] with a

null nugget justified by the small scale structure shown by the vertical variogram. The ranges of the first and second structures were 7.9 to 9 m and 34 to 40 m, respectively. A comparative analysis of the experimental variograms results in the different directions on xy-plane show some of anisotropy, because globally his behavior they do not differ from each other in the analyzed directions. Considering the ranges variation between vertical and horizontal, a geometric anisotropy can be considered in the study area and therefore representative of the entire T3 embankment sand tailings dam, because the construction process is globally repetitive.

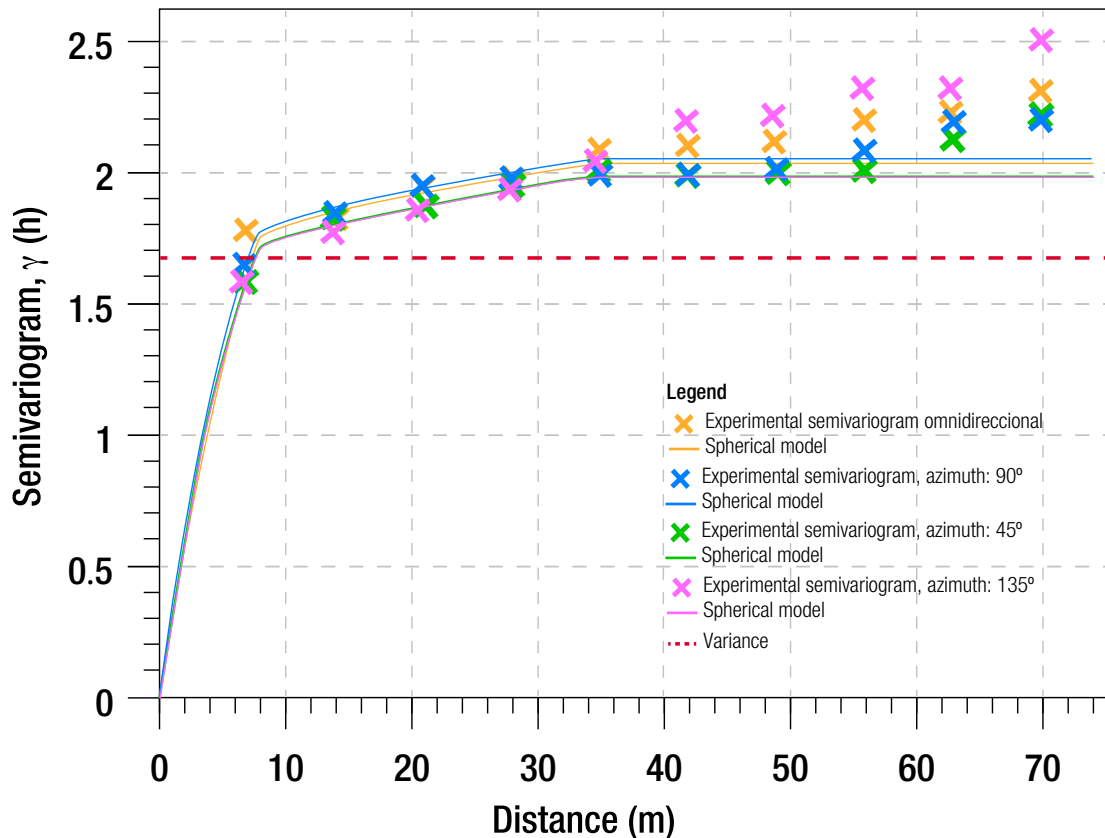


Figure 8. Experimental semivariograms and theoretical models for  $q_d$ . Horizontal analysis plane.

From the analysis of the results presented in (Table 9), it is possible to consider in a general way that the range in the vertical direction is equal to 0.6 m, while in the horizontal direction two structures at about 8 m and 33–40 m. This allows defining a global spherical variogram model for the survey grid. This variogram model (Equation (4)) is made up of three spherical structures with sills of 0.21, 0.40, and 1.62, horizontal ranges of 8.4, 36, and 40 m, and a vertical range of 0.6 m. In this case, there is no nugget effect.

$$\gamma(h) = 1.62sph(8.4, 8.4, 0.6) + 0.4sph(36, 36, 0.6) + 0.21sph(40, 40, 0.6) \quad (4)$$

#### 4.4. Using the Ordinary Kriging (OK) Method to Estimate $q_d$

The Ordinary kriging (OK) method was performed on a parallelepiped equals to the extension of study volume, subdivided in 50 cm × 50 cm × 2.5 cm blocks or cells along the x, y and z directions, respectively, using a search ellipsoid based on the dimensions of the survey grid (120 m × 45 m). A the OK with a spherical variogram model has been utilised to estimate the  $q_d$  variable according to Equation (4). The results indicate that a 95% of the estimated  $q_d$  values are equal to or lower than 4.5 MPa. This value has been used as the upper limit to facilitate graphical representation (Figure 9). Figures 10 and 11 show longitudinal profiles (xz-plane) for the first and second third of the survey grid

and medium cross-sections ( $yz$ -plane) for each test slab in terms of  $q_d$ . The following conclusions are drawn.

- The OK estimates of  $q_d$  generally reflect an anisotropic internal structure for the embankment corresponding to layers with variable thicknesses. The  $q_d$  values decrease towards the crest and increase in the downstream direction towards the foot of the embankment. These results reflect the spatial structural variability produced by the compaction process.
- All the longitudinal and cross-sectional profiles show a clear decrease in  $q_d$  at the beginning of test slab 4, which is associated with an increase in the layer thickness of the material with low  $q_d$  deposited from 0.6 to 1.2 m and matches the range assessed using the spherical model for the experimental semivariogram. This is justified by the different behaviour of the experimental vertical variogram of slab 4.

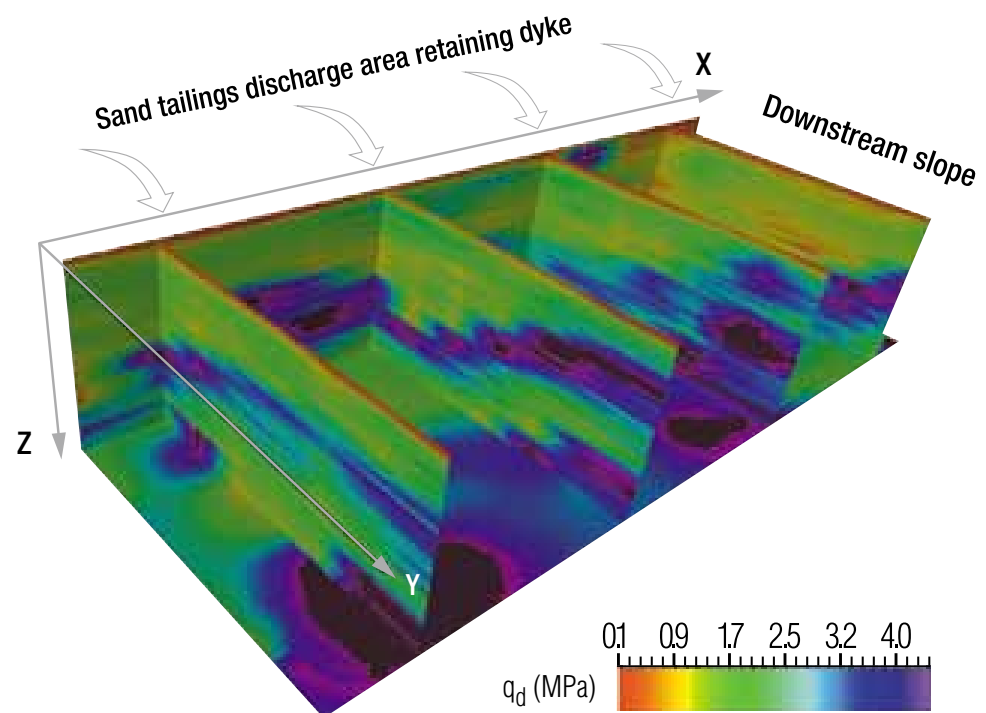


Figure 9. OK estimation of  $q_d$ . Full survey grid.

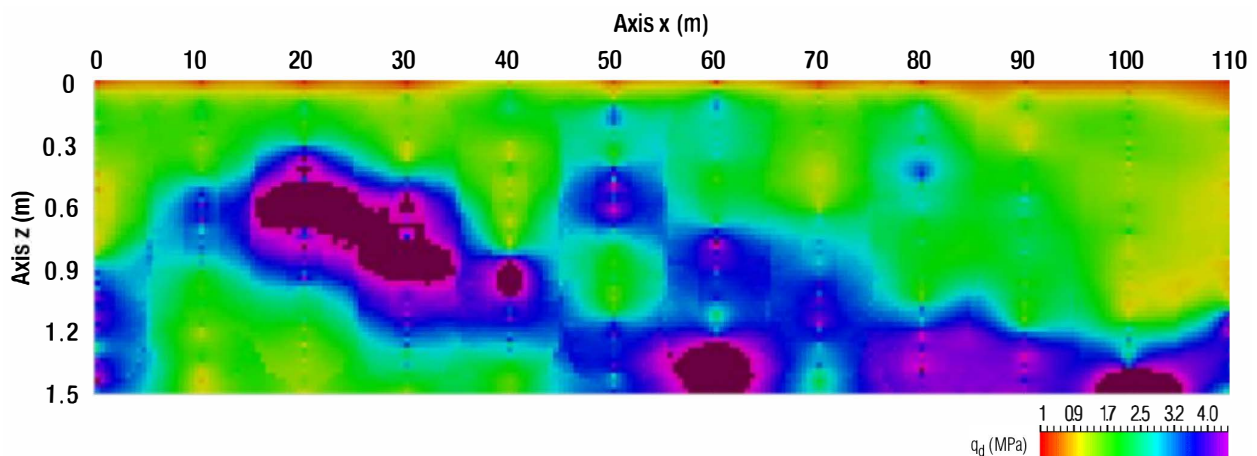
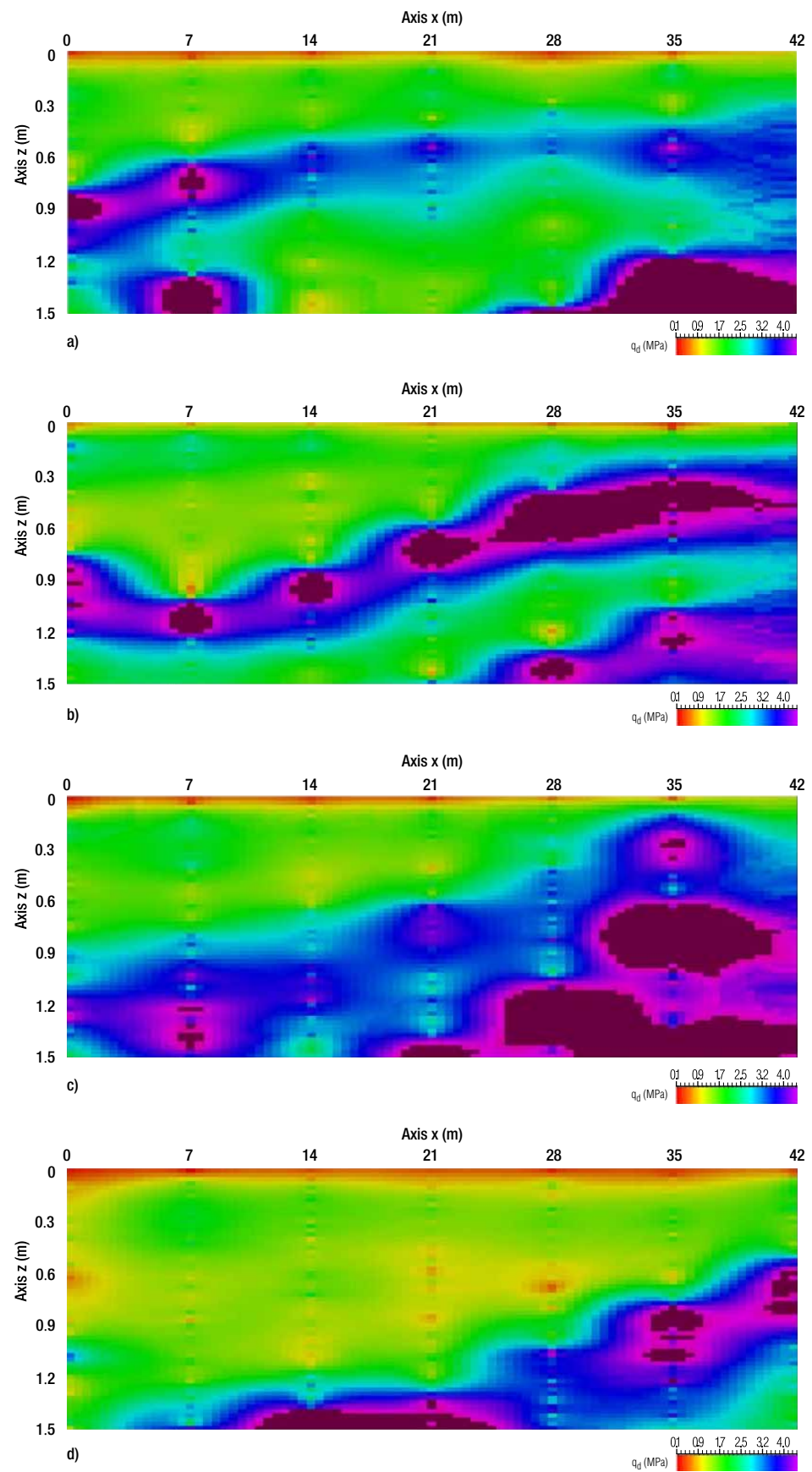
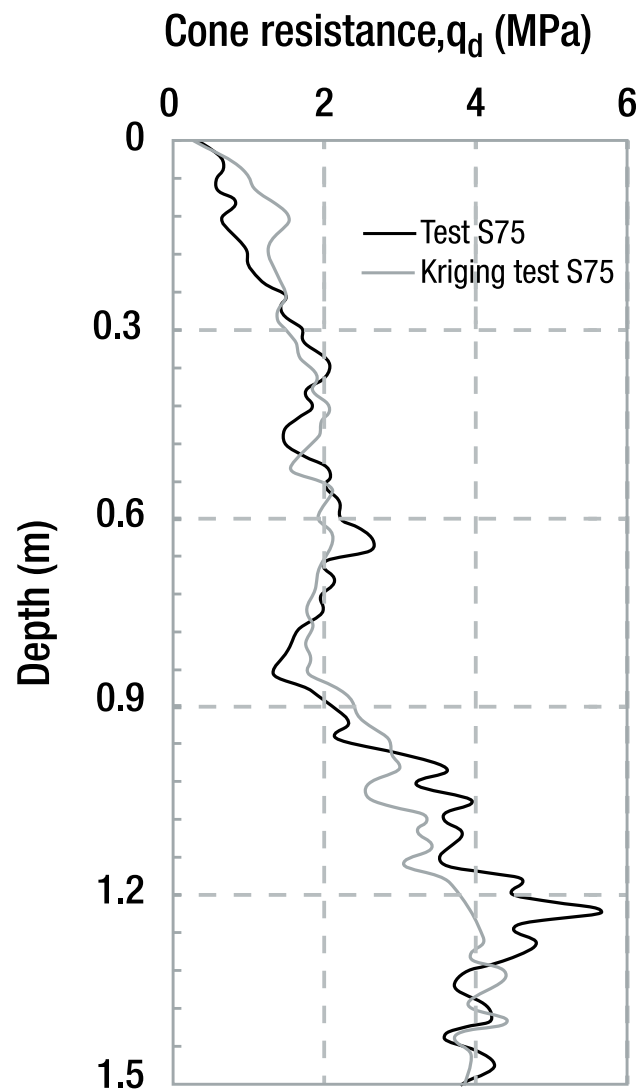


Figure 10. OK estimation of  $q_d$ .  $xz$ -plane longitudinal profile. Survey grid: First third, near the embankment dam crest.



**Figure 11.** OK estimation of  $q_d$ . yz-plane cross-sectional profile. (a) Test slab 1. (b) Test slab 2. (c) Test slab 3. (d) Test slab 4.

To compare the estimated  $q_d$  results with the results for the grid measured points and to validate the quality of the selected theoretical semivariogram model, a cross validation was performed. For this purpose, test slab 4 which has the highest number of PANDA tests points surveyed (35), was selected. Of the total, 21 PANDA tests were used, with the aim of calculating the following theoretical semivariogram parameters (Spherical model): Nugget = 0 [MPa]<sup>2</sup>; Sill = 2.86 [MPa]<sup>2</sup>; Range = 1 m. These parameters were used to perform the estimation by OK, considering the following search parameters: (i) ellipsoid dimension:  $x = 50$  m,  $y = 50$  m,  $z = 1$  m; (ii) points used in the estimation: 35 to 50 and 100 to 200. The OK results indicate a good fit between the interpolated and real values, with coefficients of determination ( $R^2$ ) of 0.82 and 0.86 for each penetrogram (Figure 12).



**Figure 12.** OK estimation of  $q_d$ . yz-plane cross-sectional profile. PANDA test 75. Test slab 4.

#### 4.5. Estimate of $\gamma_d$ and % SP

Ref. [30] conducted experimental tests on sand tailings dams derived from copper extraction and used the results to correlate  $\gamma_d$  and  $q_d$ . Thus, the experimental procedure proposed by [27] was used to determine the  $q_d/\gamma_d$  ratio for the case study case, as shown in Equation (4). Where  $q_d$  is expressed as Mpa.

$$\gamma_d = 1.11 \ln(q_d) + 17.25 (\text{kN/m}^3) \quad (5)$$

A good fit is obtained between  $\gamma_d$  estimated from  $q_d$  and  $\gamma_d$  determined using the sand-cone method shows ( $R^2 = 0.92$ ), which validates the correlation found in the present study. Vertical and horizontal theoretical semivariograms of  $\gamma_d$  estimated from  $q_d$  and the % SP compaction were derived for the full survey grid with a null nugget effect ( $Co = 0$ ) and identical ranges (Table 10). The following conclusions are drawn from the results for  $\gamma_d$  and the % SP compaction estimated using the OK method (Figure 13).

**Table 10.** Results for  $\gamma_d$  and %SP semivariogram modeling in vertical and horizontal directions for full survey grid.

Parameter	Plane of Analysis	Theoretical Model	Sill, $Co + C$	Range, [m]
$\gamma_d$	Vertical z	Spherical	0.12 [kN/m <sup>3</sup> ] <sup>2</sup>	0.7
		Spherical 1	0.11 [kN/m <sup>3</sup> ] <sup>2</sup>	5.2
	Horizontal x-y	Spherical 2	0.02 [kN/m <sup>3</sup> ] <sup>2</sup>	40.7
% SP	Vertical z	Spherical	35.82 [%] <sup>2</sup>	0.7
		Spherical 1	31.18 [%] <sup>2</sup>	5.2
		Spherical 2	5.54 [%] <sup>2</sup>	40.7

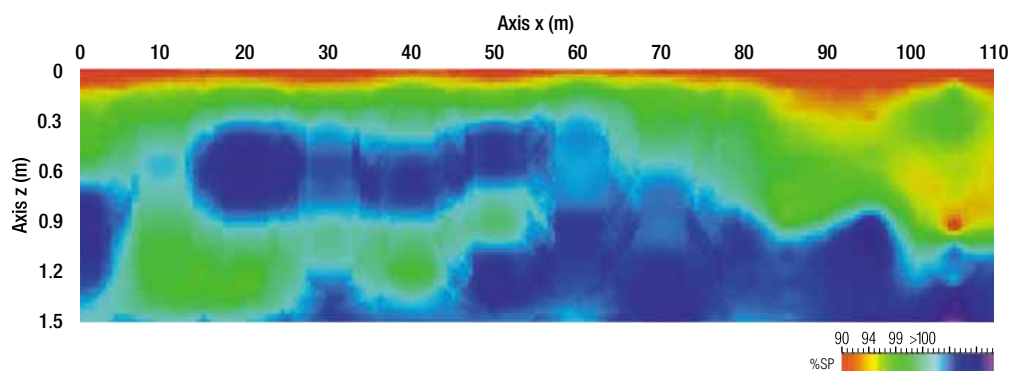


**Figure 13.** % SP compaction percentages estimated by OK. x-z plane longitudinal profile. Survey grid: second third, near the foot of the embankment.

- The sand tailings mechanically compacted into layers exhibit in situ structural variability on a spatial scale directly associated with the construction and compaction process.
- The estimated  $\gamma_d$  values range from 17 to 21.5 (kN/m<sup>3</sup>), and the % SP compaction ranges from 90 % to 100 %. These ranges are similar to the statistical analysis results for the data obtained from routine layer-by-layer compaction control.
- The models have direct practical applications for performing post-construction control of an embankment of classified sand talings dams to identify areas with weak resistance or compaction percentages below the project design values ( $SP \geq 95\%$ ) and optimize the compaction process.

### 5. Conclusions

The application of simple geostatistical techniques to the compaction control of classified sand tailings dams by the PANDA test provides an efficient and a rapid alternative to estimate spatially the variation in the degree of compaction with depth and layer thickness, considering the material (production sand tailings), and structural variability (deposition, distribution, and compaction) of an embankment, a relevant aspect not considered in

current practice, for technical and economic reasons. In this way, it is possible to perform QC checks layers recently compacted, and QA of deep layers.

The incorporation of the material and structural variability in the compaction control together with the incorporation of geostatistical models as a tool for geotechnical monitoring, constitutes an important aid for the decision-making of the operators in charge of the construction of classified sand tailings dams, periodically optimizing the compaction process in terms of the thickness of the layer a compacting and the compaction energy to be applied (type of machinery to be used and a number of operating hours). The combination of compaction control using the Lightweight PANDA Penetrometer and a simple geostatistical model allow for quick and efficient verification of the degree compaction ( $D_r$  or SP), both on the surface and in sand depth. In this way, it is possible to identify the zones that present a dilatant behavior (physically stable) in the embankment and those that show a contractive behavior with low compaction whose risk of liquefaction and slope instability in seismic conditions must be evaluated. The structural analysis has allowed having an idea of the anisotropic structure of the classified sand tailings dams, and to estimate the thickness of the internal layers, a fundamental variable for controlling the compaction of this type of deposit not measured with the commonly used control techniques.

A structural analysis of the variable  $q_d$  shows that the experimental semivariograms analyzed in different directions of the deposit can be fit using a model of three nested spherical structures. The assessed range of 0.4 to 0.7 m in the vertical direction (z-plane) is directly associated with the theoretical thickness of the compacted layers in the project (0.4 m). This range highlights the spatial structural variability of the layer thickness of the dam. This range is a key parameter for physical stability, which is typically inadequately controlled during the compaction process. The horizontal semivariograms (xy-plane) obtained in different directions (azimuth: 0°, 45°, 90°, and 135°) do not differ from each other globally and therefore do not exhibit anisotropy in the xy-plane. The second spherical model ranges from 34 to 40 m and is related to the dimensions of the test slabs composing the survey grid defined in the study area of the deposit. Confirmation of the xy-plane ranges for other classified sand tailings dams could provide an order of magnitude estimate to significantly optimize routine compaction controls that are currently performed based on only empirical criteria.

The OK estimates of the  $q_d$ ,  $\gamma_d$  and % SP variables enable the location of both weak areas with a high potential of mechanical instability and overcompacted areas, thereby facilitating evidence-based decision-making for improving the construction and compaction process.

In turn, the values determined by OK constitute an important database. Under properly recording and management procedures, these data could be processed using artificial intelligence methods (e.g., artificial neural networks) to continuously monitoring the variables that define the physical stability of these deposits over time and detect early deviations from the project design. The estimation by OK of the variable  $q_d$ , and the incorporation of the relation  $q_d/\gamma_d$  allows studying the degree of compaction of a certain area, thus being able to better identify the existence of weak areas in the embankment

Classified sand tailings dams typically have large volumetric and geometric dimensions. Thus, the size of the surface over which a given geotechnical variable of interest is estimated by OK could be increased by integrating the results from different survey methods or in situ tests (e.g., geotechnical surveys with SPT and CPTu penetration tests and near-surface geophysical methods, such as multichannel analysis of surface waves (MASW) and Microtremor Array Measurements (MAM)). A common indicator for assessing failure mechanisms (e.g., a safety factor to assess the liquefaction potential) could be developed as a tool to periodically monitor the physical stability of sand tailings dams over time during operation. Although the results obtained represent the internal structure of the embankment of a classified sand tailings dams and constitute a great help for the decision-making of the operators responsible for the operation and construction, with the objective of evaluating possible improvements in the models obtained, such as future works are proposed: (i) analyze the multi-layer structure considering a zonal anisotropy; (ii) to

perform a more robust cross-validation that validates the OK models, exploit the variance of the point-by-point estimate.

**Author Contributions:** Conceptualization, G.V. and C.B.; methodology, C.B., G.V. and A.C.; software, A.C. and M.S.; validation, G.S. and J.G.; formal analysis, A.C., G.V. and P.V. and J.P.; investigation, C.B., P.V., J.P. and J.G.; writing—original draft preparation, G.V. C.B., J.G. and G.S.; writing—review and editing, G.V., C.B., J.P., J.G. and P.V.; visualization, G.V. and J.G. All authors have read and agreed to the published version of the manuscript.

**Funding:** This research was funded by DI Interdisciplinaria Pontificia Universidad Católica de Valparaíso (PUCV), grant number 14ENI2-26905: “Inteligencia Artificial para el Monitoreo de la estabilidad de Depósitos de Relaves”.

**Data Availability Statement:** Not applicable.

**Acknowledgments:** Our sincere thanks and forever appreciation to Claude Bacconnet †, for his relevant contributions in the discipline of geotechnics, in particular to the mechanics of granular media and spatial variability of geotechnical parameters.

**Conflicts of Interest:** The authors declare no conflict of interest.

## References

1. Cochilco. *Proyección de la Producción de Cobre en Chile 2018–2029*; Cochilco: Santiago, Chile, 2019.
2. SERNAGEOMIN. Datos Públicos Depósito de Relaves. Catastro de Depósitos de Relaves en Chile. 2020. Available online: <https://www.sernageomin.cl/datos-publicos-deposito-de-relaves/> (accessed on 5 November 2022).
3. Villavicencio, G.; Espinace, R.; Palma, J.; Fourie, A.; Valenzuela, P. Failures of sand tailings dams in a highly seismic country. *Can. Geotech. J.* **2014**, *51*, 449–464. 10.1139/cgj-2013-0142. [CrossRef]
4. Villavicencio, G.; Breul, P.; Bacconnet, C.; Fourie, A.; Espinace, R.A. Liquefaction potential of sand tailings dams evaluated using a probabilistic interpretation of estimated in-situ relative density. *Rev. Constr.* **2016**, *15*, 9–18. [CrossRef]
5. NF P94-105; Grounds: Investigation and Testing Measuring Compaction Quality. Method Using Variable Energy Dynamic Penetrometer. Penetrometer Calibration Principle and Method. Processing Results. Interpretation. AFNOR.M: La Plaine Saint-Denis, France, 2012.
6. Nch 3261-12; Tailings Deposits-Control of Compaction with Light Dynamic Penetrometer; INN: Santiago, Chile, 2012.
7. ASTM D1556/D1556M-15e1; Standard Test Method for Density and Unit Weight of Soil in Place by Sand-Cone Method. ASTM: West Conshohocken, PA, USA, 2015.
8. Vennapusa, P.K.R.; White, D.J.; Morris, M.D. Geostatistical analysis for spatially referenced roller-integrated compaction measurements. *J. Geotech. Geoenviron. Eng.* **2010**, *136*, 813–822. [CrossRef]
9. Soulié, M.; Montes, P.; Silvestri, V. Modelling spatial variability of soil parameters. *Can. Geotech. J.* **1990**, *27*, 617–630. [CrossRef]
10. Sitharam, T.G.; Samui, P. Geostatistical modelling of spatial and depth variability of SPT data for Bangalore. *Geomech. Geoenviron.* **2007**, *2*, 307–316. [CrossRef]
11. Altun, S.; Göktepe, A.; Sezer, A. Geostatistical interpolation for modelling SPT data in northern Izmir. *Sadhana* **2013**, *38*, 1451–1468. [CrossRef]
12. Costa, Y.; Cunha, E.; Costa, C.; Pereira, A. Correlations between SPT and CPT data for a sedimentary tropical silty sand deposit in Brazil. In *Geotechnical and Geophysical Site Characterisation 5*; Lehane, B.M., Acosta-Martínez, H.E., Kelly, R., Eds.; Australian Geomechanics Society; Sydney, Australia, 2016; pp. 407–412.
13. Fisonga, M.; Wang, F.; Mutambo, V. The estimation of sampling density in improving geostatistical prediction for geotechnical characterization. *Int. J. Geotech. Eng.* **2018**, *15*, 724–731. [CrossRef]
14. Kim, H.-S.; Kim, H.-K. Optimizing site-specific geostatistics to improve geotechnical spatial information in Seoul, Korea. *Arab. J. Geosci.* **2019**, *12*, 104. [CrossRef]
15. Kim, M.; Kim, H.-S.; Chung, C.-K. A Three-Dimensional geotechnical spatial modeling method for borehole dataset using optimization of geostatistical approaches. *KSCE J. Civ. Eng.* **2020**, *24*, 778–793. [CrossRef]
16. ASTM D2922-05; Standard Test Methods for Density of Soil and Soil-Aggregate in Place by Nuclear Methods. ASTM: West Conshohocken, PA, USA, 2005.
17. Valenzuela, L. Design, construction, operation and the effect of fines content and permeability on the seismic performance of tailings sand dams in Chile. *Obras Proy.* **2016**, *19*, 6–22. [CrossRef]
18. Verdugo, R. Compactación de relaves. In *Proceedings of the IV Chilean Congress of Geotechnical Engineering*, Valparaíso, Chile, 1997.
19. Barrera, S.; Valenzuela, L.; Campaña, J. Sand tailings dams: Design, construction and operation. In *Tailings and Mine Waste 2011*; Academic Press: Vancouver, BC, Canada, 2011; p. 13.
20. Troncoso, J. *Envejecimiento y Estabilidad sísmica de un Depósito de Residuos Minerales en Condición de Abandono*; Apuntes de Ingeniería: Santiago, Chile, 1986; pp.147–158.

21. Bhanbhro, R. Mechanical Behavior of Tailings: Laboratory Tests from a Swedish Tailings Dam. Ph.D. Thesis, Luleå University of Technology, Luleå, Sweden, 2017.
22. Martin, T.E.; McRoberts, E.C. Some considerations in the stability analysis of upstream tailings dams. In Proceedings of the Sixth International Conference on Tailings And Mine Waste, Fort Collins, CO, USA, 24–27 January 1999; AA Balkema: Rotterdam, The Netherlands, 1999; Volume 99, pp. 287–302.
23. Verdugo, R. Seismic performance of slopes and earth and tailings dams (2010 Maule Earthquake). In Proceedings of the Fifth International Conference on Geotechnical Earthquake Engineering (5-ICEGE), Santiago, Chile, 10–13 January 2011.
24. Sernageomin. Guía Metodológica para Evaluación de la Estabilidad Física de Instalaciones Mineras Remanentes. 2018. Available online: <https://www.sernageomin.cl/wp-content/uploads/2019/06/GUIA-METODOLOGICA.pdf> (accessed on 3 June 2022).
25. Cassan, M. *Les Essais In Situ en Mécanique des Sols. Volume 1: Réalisation et Interpretation*, 2nd ed.; Eyrolles: Paris, France, 1988.
26. Gourvès, R.; Barjot, R. The Panda ultralight dynamic penetrometer. In Proceedings of the 11th European Conference on Soil Mechanics Foundation, San Francisco, CA, USA, 12–16 August 1985; Danish Geotechnical Society: Copenhagen, Denmark, 1995; pp. 83–88.
27. Benz, M.A. *Mesures Dynamiques lors du Battage du Pénétrömètre Panda 2*; University Blaise Pascal: Clermont Ferrand, France, 2009.
28. Villavicencio, G.; Suazo, G.; Zúñiga, R.; Valenzuela, P. Effects of Soil Conditions on the Cone Resistance of Lightweight Penetrometers. *J. Geotech. Geoenviron. Eng.* **2021**, *147*, 04021049. [[CrossRef](#)]
29. Chaigneau, L. *Caractérisation des Milieux Granulaires de Surface à l'Aide d'un Pénéromètre*; Université Blaise Pascal: Clermont Ferrand, France, 2001.
30. Villavicencio, G.; Breul, P.; Espinace, R.; Valenzuela, P. Control de compactación con penetrómetros ligeros en tranques de relaves, considerando su variabilidad material y estructural. *Rev. Constr.* **2012**, *11*, 119–133. [[CrossRef](#)]
31. Cambou, B. *Mécanique des Milieux Granulaires: L'Approche Microstructurale. Rhéologie des Géomatériaux*; Darve, F., Ed.; Presse E.N.P.C: Paris, France 1987; pp. 261–278.
32. Biarez, J.; Favre J.L. *Statistical Estimation and Extrapolation from Observations. Reports of Organisers*; IX ICSMFE: Tokyo, Japan, 1977; Volume 3, pp. 505–509.
33. Favre, J.L. Milieu Continu et Milieu Discontinu: Mesure Statistique Indirecte des Paramètres rhéologiques et Approche Probabiliste de la Sécurité. Ph.D. Thesis, Université Pierre et Maire Curie, Paris, France, 1980.
34. Salgado, R.; Mitchell, J.K.; Jamiolkowski, M. Cavity expansion and penetration resistance in sand. *J. Geotech. Geoenviron. Eng.* **1997**, *123*, 878–888. [[CrossRef](#)]
35. Rahim, A.; Prasad, S.Y.; George, K. Dynamic Cone Penetration Resistance of Soils-Theory and Evaluation. In Proceedings of the Geo-Trans 2004 Conference, Los Angeles, CA, USA, 27–31 July 2004.
36. Arnaouti, S.; Angelides, D.; Chatzigogos, T.; Pytel, W. Variability of Soil Strength Parameters and its Effect on the Slope Stability of the Želazny Most Tailing Dam. *Int. J. Geol. Environ. Eng.* **2012**, *6*, 415–421. [[CrossRef](#)]
37. Hamade, T.; Mitri, H. Reliability-based approach to the geotechnical design of tailings dams. *Int. J. Mining Reclam. Environ.* **2013**, *27*, 377–392. [[CrossRef](#)]
38. Bhanbhro, R. *Mechanical Properties of Tailings: Basic Description of a Tailings Material from Sweden*; Luleå University of Technology: Luleå, Sweden, 2014.
39. Hu, L.; Wu, H.; Zhang, L.; Zhang, P.; Wen, Q. Geotechnical properties of mine tailings. *J. Mater. Civ. Eng.* **2017**, *29*, 04016220. [[CrossRef](#)]
40. Villavicencio, A.G.; Breul, P.; Bacconnet, C.; Boissier, D.; Espinace, A.R. Estimation of the Variability of Tailings Dams Properties in Order to Perform Probabilistic Assessment. *Geotech. Geol. Eng.* **2011**, *29*, 1073–1084. [[CrossRef](#)]
41. Troncoso, J.; Garcés, E. Ageing effects in the shear modulus of soils. *Soil. Dyn. Earthq.* **2000**, *19*, 595–601. [[CrossRef](#)]
42. Paikowsky, S.; Birgisson, B.; McVay, M.; Nguyen, T.; Kuo, C.; Baecher, G.; Ayyub, B.; Stenersen, K.; OíMalley, K.; Chernauskas, L.; et al. *Load and Resistance Factor Design (LRFD) for Deep Foundations*; Transportation Research Board: Washington, DC, USA, 2004.
43. Juárez-Camarena, M.; Auvinet-Guichard, G.; Méndez-Sánchez, E. Geotechnical zoning of Mexico Valley subsoil. *Ing. Investig. Tecnol.* **2016**, *17*, 297–308. [[CrossRef](#)]
44. Journel, A.; Huijbregts, C. *Mining Geostatistics*; Academic Press: London, UK; New York, NY, USA, 1978.
45. Matheron, G. *Traité de Geostatistique Appliquée, Volumen 1. Mémoires du BRGM, 14*; Technip: Paris, France, 1962.
46. Matheron, G. *The Theory of Regionalized Variables and its Applications. Volumen 5. Les Cahiers du Centre de Morphologie Mathématique de Fontainebleau*; École Nationale Supérieure des Mines: Paris, France, 1971.
47. Baczkowski, A.J.; Clark, I. Practical Geostatistics. *J. R. Stat. Soc. Ser.* **1981**, *144*, 537. [[CrossRef](#)]
48. Hohn, M.E. An Introduction to Applied Geostatistics. *Comput. Geosci.* **1991**, *17*, 471–473. [[CrossRef](#)]
49. Burgess, T.M.; Webster, R. Optimal interpolation and isarithmic mapping of soil properties. I. The semi-variogram and punctual kriging. *J. Soil Sci.* **1980**, *31*, 315–331. [[CrossRef](#)]
50. De Rubeis, V. Application of kriging technique to seismic intensity data. *Bull. Seismol. Soc. Am.* **2007**, *95*, 540–548. [[CrossRef](#)]
51. Deplagne, F.; Bacconnet, C. Analyse structural d'une digue en argile. *Cah. Géostat.* **1993**, *3*, 188–191.
52. Villavicencio, G. *Méthodologie pour Évaluer la Stabilité Mécanique des Barrages de Résidus Miniers*. Ph.D. Thesis, University Blaise Pascal, Clermont Ferrand, France, 2009

53. Raspa, G.; Innocenti, C.; Marconi, F.; Mumelter, E.; Salmeri, A. Evaluation of an Automatic Procedure Based on Geostatistical Methods for the Characterization of Contaminated Sediments. In *GeoENV VI-Geostatistics for Environmental Applications*; Soares, A., Pereira, M., Dimitrakopoulos, R., Eds.; Springer: New York, NY, USA, 2008; pp. 421–441.
54. Vessia, G.; Di Curzio, D.; Castrignanò, A. Modeling 3D soil lithotypes variability through geostatistical data fusion of CPT parameters. *Sci. Total Environ.* **2020**, *698*, 134340. [[CrossRef](#)] [[PubMed](#)]
55. Alfaro, M. Estimación de Recursos Mineros. Available online: [cg.ensmp.fr/bibliotheque/public/ALFARO\\_Cours\\_00606.pdf](http://cg.ensmp.fr/bibliotheque/public/ALFARO_Cours_00606.pdf) (accessed on 2 November 2020).